Atmos. Chem. Phys. Discuss., 11, 7757–7780, 2011
www.atmos-chem-phys-discuss.net/11/7757/2011/
doi:10.5194/acpd-11-7757-2011

Atmospheric Chemistry and Physics Discussions

Sulphur dioxide as a volcanic ash proxy during the April–May 2010 eruption of Eyjafjallajökull Volcano, Iceland

H. E. Thomas[1] **and A. J. Prata**[2]

[1]Department of Geological Engineering and Sciences, Michigan Technological University, Houghton, MI, USA
[2]Nordic Institute for Air Research (NILU), Kjeller, Norway

Received: 18 February 2011 – Accepted: 25 February 2011 – Published: 7 March 2011

Correspondence to: H. E. Thomas (hethomas@mtu.edu)

Published by Copernicus Publications on behalf of the European Geosciences Union.

Abstract

The volcanic ash cloud from the eruption of Eyjafjallajökull volcano in April and May 2010 resulted in unprecedented disruption to air traffic in Western Europe causing significant monetary loses and highlighting the importance of efficient volcanic cloud monitoring. The feasibility of using SO_2 as a tracer for the ash released during the eruption is investigated here through comparison of ash retrievals from the Spinning Enhanced Visible and Infrared Imager (SEVIRI) with SO_2 measurements from a number of infrared and ultraviolet satellite-based sensors. Results demonstrate that the eruption can be divided into an initial ash-rich phase, a lower intensity middle phase and a final phase where considerably greater quantities of both ash and SO_2 were released. Comparisons of ash-SO_2 dispersion indicate that despite frequent collocation of the two species, there are a number of instances throughout the eruption where separation is observed. This separation occurs vertically due to the more rapid settling rate of ash compared to SO_2, horizontally through wind shear and temporally through volcanological controls on eruption style. The potential for the two species to be dispersed independently has consequences in terms of aircraft hazard mitigation and highlights the importance of monitoring both species concurrently.

1 Introduction

The Eyjafjallajökull volcano, Iceland (63.63° N, 19.62153° W; 1666 m a.s.l.) erupted explosively on 14 April 2010 and continued to emit ash and gas until 24 May. Despite the relatively modest size of the eruption, the prevailing wind conditions to the south-east resulted in the eruption having a considerable impact upon aviation in Europe. The closure of the majority of European airspace from 17–19 April alone led to an estimated loss of $1.7 billion to the aviation industry (IATA, 2010). One of the most significant consequences of the eruption was the change in flight safety policy from zero tolerance to the introduction of ash concentration thresholds (CAA, 2010). Areas of low

ACPD
11, 7757–7780, 2011

($<2\times10^{-3}$ g m^{-3}), medium (2–4 $\times$ 10^{-3} g m^{-3}) and high ($>4\times10^{-3}$ g m^{-3}) ash concentration have since been defined by the International Civil Aviation Organization (ICAO) to determine where flight is allowable (low), allowable under certain specific conditions (medium) or prohibited (high) (ICAO, 2010).

Ash encounters with aircraft are not uncommon and at least 94 confirmed incidents were reported from 1953–2009 (Guffanti et al., 2010), where the most serious have only narrowly avoided catastrophe due to engine flame outs. With the current rapid rate of air traffic growth (ESCAP, 2005) there is the potential for many more such incidents and it is the responsibility of the Volcanic Ash Advisory Centers (VAACs) to provide advisories to the aviation industry through the effective modelling and monitoring of eruption clouds. Throughout the Eyjafjallajökull eruption, the London VAAC at the UK Met Office was responsible for producing model predictions for the location of the ash cloud. Following the introduction of a quantitative ash threshold, predictions of ash concentration were also reported in order to advise the aviation authorities throughout the six-week eruption period. However, reliance on models alone is problematic due to the nature of volcanological and meteorological conditions which can cause rapid and unexpected changes in ash distribution. Satellite remote sensing provides means by which model results can be validated in near real-time and subsequently used to improve the accuracy of outputs (e.g. Stohl et al., 2011) thereby allowing volcanic cloud prediction with greater certainty.

Explosive magmatic eruptions typically emit both ash and sulphur dioxide (SO_2) concurrently. As SO_2 is generally easier to detect with space-based instruments (Eckhardt et al., 2008), it is frequently used as a proxy for ash (Carn et al., 2009). Furthermore, SO_2 clouds may also be associated with very fine ash particles which are difficult to detect using remote sensing methods, but could still pose a hazard to aircraft. While volcanic ash primarily affects aircraft engines, rapid conversion of SO_2 in the atmosphere to sulphuric acid aerosols (sulphate) can cause an increase in corrosion rates of aircraft compressor blades (Swadzba et al., 1996). The presence of sulphate aerosols at cruising altitudes can also result in rapid crazing of acrylic windows and a number

ACPD
11, 7757–7780, 2011

of cases of airframe damage have been attributed to aerosol from the eruptions of El Chichón, Mexico in 1982 and Pinatubo in 1991 (Bernard and Rose, 1990; Casadevall et al., 1996).

Although the two species are usually released concurrently, separation may occur through wind shear and particle settling (Prata and Kerkmann, 2007). Furthermore, the success of volcanic ash retrievals using infrared algorithms are highly dependent on water and ice content of the cloud, which can mask the ash signal in high quantities (Pavolonis et al., 2006). As the Eyjafjallajökull eruption was sub-glacial, this is likely to play a significant role in ash cloud detection due to the elevated water vapour in the cloud.

In this study we assess the validity of using SO_2 as a tracer for volcanic ash for the case of the Eyjafjallajökull eruption by comparing retrievals of ash concentration from the geosynchronous Meteosat Second Generation (MSG) Spinning Enhanced Visible and Infrared Imager (SEVIRI), with additional retrievals of sulphur dioxide from a range of satellite-based sensors on polar orbiting platforms. The Global Ozone Monitoring Instrument 2 (GOME-2) and the Infrared Atmospheric Sounding Interferometer (IASI) onboard the Eumetsat MetOp-A platform, the Ozone Monitoring Instrument (OMI) on the NASA Aura satellite and the Atmospheric Infrared Radiation Sounder (AIRS) on the NASA Aqua platform are all capable of detecting volcanic SO_2 with varying spatial, spectral and temporal resolutions (Table 1). The use of a number of sensors allows for a greater wealth of information about the plume altitude and distribution to be determined than through using just one sensor alone (Thomas et al., 2011).

The Cloud-Aerosol Lidar with Orthogonal Polarisation (CALIOP) spaceborne lidar, on board the CALIPSO platform has also been used to provide information about aerosol altitude and vertical distribution of ash and aerosol particles. Also utilised are the European Centre for Medium-Range Weather Forecasts (ECMWF) interim re-analysis data, for comparison of cloud transportation with local wind fields. These data contain the u and v wind velocity components at a 1° resolution from sea level up to 0.1 hPa at six hourly intervals (Berrisford et al., 2009). Satellite observations are

ACPD
11, 7757–7780, 2011

compared to the prediction issued by the London VAAC using the operational dispersion model, NAME III (Numerical Atmospheric – dispersion Modelling Environment) (Jones et al., 2007). Predictions were released on a six-hourly basis for the north Atlantic region and are available online from http://www.metoffice.gov.uk/aviation/vaac/.

2 Methodology

2.1 Ash retrievals

The retrieval of volcanic ash for the SEVIRI instrument is based on the difference in brightness temperature between channels 9 (10.8 µm) and 10 (12 µm) (Prata, 1989a, b). The refractive indices of the ash particles are predetermined and are input into a Mie scattering code using a range of particle sizes and wavelengths. A discrete ordinates model (DOM) (Stamnes and Swanson, 1981) and a look up table for the range of top of atmosphere (TOA) brightness temperatures for each of the two channels are generated. These values are then compared with the atmospherically corrected satellite data to derive the optical depth and ash properties, which are used to compute the total ash mass of each pixel (Wen and Rose, 1994; Prata and Grant, 2001). The retrieval scheme was applied to all images acquired between 14 April and 25 May to generate ash maps for every 15 min interval during the eruption period, resulting in a total of 3936 images. The total mass was also calculated for each scene by summing up the mass loadings and multiplying by the total area of affected pixels.

2.2 SO_2 retrievals

The retrieval of the partial column of SO_2 from AIRS uses channels situated across the 7.3 µm absorption band and follows the method proposed by Prata and Bernardo (2007). The retrieval is a two-step process: in the first step a correlation method is used to identify the band by correlating the spectral shape with a library

ACPD
11, 7757–7780, 2011

band shape. In the second step an optimal estimation technique (Rodgers, 2000) is used to retrieve the SO_2 in slabs of 2 km thickness. These are then summed to provide a partial column SO_2 amount. Typical errors range from ±3 Dobson Units (DU) to ±6 DU, depending on the amount of water vapour present in the atmosphere and in the cloud. The retrieval is limited by several factors, including thermal contrast (the temperature difference between the SO_2 cloud and the surface below), the amount of water vapour, which usually restricts the retrieval to SO_2 that resides above 3 km or so, and saturation of the band. This last effect is not evident in the AIRS retrievals for Eyjafjallajökull, which occurs when the cloud is optically thick and the spectra appear flat. These limitations must be borne in mind when making comparisons with estimates from other sensors (e.g. OMI and GOME-2).

Retrieval of SO_2 from IASI is described by Clarisse et al. (2008). Like AIRS, IASI is sensitive to SO_2 in the middle- to upper-troposphere and lower stratosphere, with sensitivity limited by the water vapour content of the atmosphere and clouds. In principle, the better spectral resolution and slightly better signal-to-noise of IASI compared to AIRS provides better SO_2 retrievals, but so far a thorough validation and inter comparison of retrievals has not been undertaken.

The ultraviolet (UV) sensors OMI and GOME measure the total backscattered solar irradiance from the Earth's surface and the SO_2 total column is computed using the Beer-Bouguer-Lambert law. Absorption due to SO_2 is differentiated from that of ozone by using measurements at multiple wavelengths (Kerr, 1980; Krueger, 1983; Krueger et al., 1995). OMI SO_2 data are derived using the linear fit algorithm of Yang et al. (2007) and are retrieved as the OMSO2 product from http://mirador.gsfc.nasa.gov/. GOME-2 products are computed using a differential optical absorption spectroscopy (DOAS) algorithm (Eisinger and Burrows, 1998) and are provided online at http://sacs.aeronomie.be/. As these UV sensors measure the total column SO_2, using radiance which has been reflected from the surface of the Earth, SO_2 at low altitude can also be detected. SO_2 data from all four sensors were analysed for the period 14 April–24 May and images containing SO_2 were compared with the nearest time-coincident

ACPD
11, 7757–7780, 2011

ash retrieval from SEVIRI along with information from the CALIPSO lidar where available (browse images v. 3.01 acquired from http://www-calipso.larc.nasa.gov/).

3 Observations and discussion

3.1 Eruption chronology

After a number of weeks of heightened seismic activity and a fissure eruption at Fimmvörðuháls lasting approximately three weeks, the summit eruption of Eyjafjallajökull began on 14 April, sending ash clouds to more than 8 km altitude (BGS, 2010). From 19 April until early May, activity continued with a lower intensity with plume altitudes reaching an average height of 4 km (Smithsonian Institution, 2010). In early May the plume was reported to be darker and wider than during the past three weeks showing a rapid increase in ash discharge rate with both lava-producing and explosive phases (Icelandic Met Office, 2010; Smithsonian Institution, 2010). On 4 May the explosive activity at Eyjafjallajökull was seen to gain intensity, with observations estimating the plume altitude at 6 km (Hjaltadóttir et al., 2010). The volcano continued to emit ash and gas up until 24 May when the eruption ended. These different phases of the eruption can be clearly distinguished using satellite data. Figure 1 shows the total ash tonnage as measured by SEVIRI for each image throughout the eruption period, along with the OMI and AIRS SO_2 tonnages for overpasses which captured the entire cloud region (so that results were not biased by overpasses where only part of the plume was imaged). The first phase is dominated by ash with very little SO_2 detected by either AIRS or OMI which is consistent with the interglacial nature of the eruption. The middle phase shows little in the way of ash or SO_2 detected by the satellite based sensors, indicating that the explosions at this time were much less ash rich and likely dominated by water vapour, along with a small amount of low altitude SO_2, as detected by OMI. The final phase is indicative of a magmatic eruption releasing both SO_2 and ash in two distinct phases, peaking on 9 May and 15 May.

ACPD
11, 7757–7780, 2011

3.2 15 and 16 April

During the first phase, SO_2 clouds were difficult to distinguish in the AIRS and IASI imagery, due to their low altitude and concentration, although some SO_2 was detected by the UV sensors on a number of days. Figure 2 shows the near-coincident SEVIRI ash retrievals with the OMI and GOME-2 SO_2 retrievals on 15 and 16 April. The images show some spatial disparity between regions of SO_2 and ash as measured by the instruments. On 15 April, the SO_2 cloud extends further to the east than the majority of the ash and the relative locations of ash and SO_2 show that there is little gas associated with the area of densest ash. Conversely, the most concentrated area of SO_2 to the east does not appear to have high ash concentrations associated with it. The images from GOME-2 and SEVIRI on 16 April show a general collocation of the ash and gas, although the GOME-2 imagery does detect a noteworthy SO_2 cloud over Finland that is larger than the corresponding region of ash. Through tracing the clouds' evolution over time, this SO_2 was originally associated with the ash cloud visible in the SEVIRI image at 12:00 UTC (Fig. 2a), and was erupted at approximately 08:30 on 15 April. It is possible that during the 24 hours of transportation in the atmosphere the majority of the large ash particles will have settled out, leaving just SO_2 and fine ash in suspension. Due to the intra-glacial nature of the eruption in the early explosive phase, rapid ash fall-out is possible as the high water and ice content of the cloud would facilitate the removal of ash by gravity (Rose et al., 1995).

Comparison with the VAAC model prediction shows that both the ash and SO_2 are within the region originally forecasted to contain ash. However, these images also demonstrate that the region delineated by the VAAC model is much larger than the area of volcanic species detected by any of the sensors. This conservative estimate of the cloud dispersion could have benefited from the additional information provided by the satellite data in order to allow aircraft operation over the regions which are clearly not affected by the volcanic material.

ACPD
11, 7757–7780, 2011

3.3 4 May

Retrievals from 4 May demonstrate the advantage of using SO_2 retrievals in order to locate the cloud where ash retrievals may fail (Fig. 3). At this time, the eruption was beginning to re-intensify, although the SEVIRI ash retrievals for this day do not indicate the presence of a sustained ash plume. The ash is visible in the MODIS visible imagery (Fig. 3c), and can also be identified subjectively in time-series of SEVIRI brightness temperature imagery. However, subjective interpretation cannot be automated for rapid detection and does not permit numerical estimates of concentration, which have now become important in terms of defining regions of aircraft hazard. The SO_2 cloud in this case is evidently imaged by the two UV sensors and is therefore assumed to be at low altitude (<6 km) over the United Kingdom as it remains undetected by both AIRS and IASI. The OMI aerosol index (AI) is a measure of absorption by aerosols at 354 and 388 nm, including volcanic ash (Torres et al., 2007). In this case the OMI AI data is only able to detect the densest region of ash close to the vent and like the IR sensors, is unable to distinguish the majority of the cloud. The low plume altitude and cloudy meteorological conditions, as indicated by the MODIS visible image, are likely to have limited the ability of the ash retrieval algorithms to effectively identify the ash cloud. The spatial comparison with the output from the London VAAC model for this day shows that the region of SO_2 actually extends further to the east of the designated no-fly zone which may have implications for aircraft operating in this region.

3.4 7 May

On 7 May the SO_2 retrieval from the morning overpass of IASI compared with the SEVIRI ash indicates that the two species are well collocated (Fig. 4). However, the GOME-2 SO_2 imagery indicates a segment of SO_2 which is further to the north and west than the ash. This separation is observed to remain at 14:30 UTC when the AIRS and OMI overpasses occurred (Fig. 5a–c). The separated part of the cloud is thought to be below about 6 km altitude, as very little SO_2 is detected by IASI and AIRS.

ACPD
11, 7757–7780, 2011

The CALIOP Lidar track, coincident with the AIRS and OMI afternoon overpasses on the 7 May also intersected the volcanic cloud and can be used to infer the process causing the ash and gas separation (Fig. 5). The data indicate that the portion of the cloud through which the lidar track passes, may actually be distributed over several altitude levels, between approximately 3 and 9 km. A second feature to the north, also likely to be associated with volcanic aerosol forms a thinner layer around 5 km. This layer shows a low attenuated colour ratio (ACR) and also low depolarisation, which is indicative of the smaller sulphate aerosol particles as opposed to ash. It therefore seems likely that this layer represents the eastern edge of the separated SO_2 cloud. In order to confirm this hypothesis, the European Centre for Medium-Range Weather Forecasts (ECMWF) reanalysis wind field data are also evaluated (Fig. 6). These data demonstrate that although wind direction is fairly consistent around 165° over all altitudes, the wind speed between 600 hPa and 400 hPa (ca. 4–6 km) is higher than that immediately above and below, which is likely to be causing the observed shearing to the north-west.

3.5 13 May

During the late afternoon of 13 May the cloud shows a change in plume direction from predominantly easterly and northerly to south-easterly. Figure 7 shows the ash retrieval from SEVIRI from 12:30 UTC on the 13 May until 03:30 on 14 May which demonstrates this change in direction. The coincident OMI, IASI and AIRS SO_2 retrievals for this period are also shown. The satellite data indicates that both species are changing direction, although the AIRS and IASI images suggest that the concentration of SO_2 moving south exceeds that going north, whereas ash concentrations are approximately equal. Figure 8 shows the ECMWF wind fields at approximately 10 km and 3 km at 18:00 UTC on 13 May. The southerly component of the wind at 10 km is much stronger than at 3 km and the opposite is true for the winds which are moving the cloud to the north-west. It therefore seems likely that the southward moving ash and gas are at a higher altitude than the cloud moving north.

ACPD
11, 7757–7780, 2011

4 Conclusions

The ash and gas cloud released during the eruption of Eyjafjallajökull was imaged throughout the period of 15 April–24 May by a number of satellite based sensors. Ash retrievals from the MSG SEVIRI instrument at 15 minute intervals and SO_2 measurements from OMI, GOME-2, IASI and AIRS are all useful in detecting and locating the cloud which shows highly variable dispersion over the nearly six week period. This work has demonstrated that through comparison of coincident measurements of ash and SO_2, the validity of using SO_2 as a tracer for the motion of ash in this instance can be evaluated. We have shown that although for the majority of the eruption the gas and ash were collocated there are a number of instances where the two species do vary spatially. Separation due to the differential residence times of ash and SO_2 in the atmosphere results in the SO_2 cloud travelling further distances than the ash. This has important consequences for the aviation industry as it is likely some of the finest ash particles are remnant in the cloud. Separation due to wind shear has also been seen to occur on some days. Shearing can affect one species more than the other when vertical separation has taken place either due to the initial eruption style or through differential rates of particle settling. Finally, we observe an instance where the SO_2 retrievals from the UV sensors detect a considerable gas cloud which the ash algorithm fails to record. In this instance, the existing meteorology has significantly limited the effectiveness of the algorithm and the more sensitive UV algorithms allow the plume to be detected.

We conclude that the monitoring of both species is important during volcanic eruption episodes in order to provide the most accurate representation of the cloud in both time and space. The use of the polar orbiting UV sensors, although lacking the temporal frequency of SEVIRI, allow for the more sensitive detection of SO_2 which can, as has been shown here, detect the volcanic cloud where the ash algorithm cannot.

ACPD
11, 7757–7780, 2011

Acknowledgements. The authors acknowledge Eumetsat for financial support for this research. We also thank L. Clarisse (ULB) for provision of IASI data, S.Carn (MTU) for OMI data and discussion of CALIPSO data, S. Eckhardt (NILU) for acquiring the 3-D wind field data from ECMWF and S. Murray (UoB) for proof reading.

References

Bernard, A. and Rose, W.: The injection of sulfuric acid aerosols in the stratosphere by the El Chichón volcano and its related hazards to the international air traffic, Nat. Hazards, 3, 59–67, doi:10.1007/bf00144974, 1990.

Berrisford, P. D., Dee, K., Fielding, M., Fuentes, P., Kallberg, S., Kobayashi, S., and Uppala, S.: The ERA-Interim archive, Report Series. 1, European Centre for Medium-Range Weather Forecasts, Shinfield Park, Reading, 2009.

BGS: Changing eruption styles at Eyjafjallajökull in Iceland: http://www.bgs.ac.uk/research/highlights/changingEruptionStyles.html, last access: 17 February 2011, 2010.

CAA: Rationale for the removal of the current volcanic ash buffer zone, v.1.1, Civil Aviation Authority, 2010.

Carn, S., Krueger, A., Krotkov, N., Yang, K., and Evans, K.: Tracking volcanic sulfur dioxide clouds for aviation hazard mitigation, Nat. Hazards, 51, 325–343, doi:10.1007/s11069-008-9228-4, 2009.

Casadevall, T. J., Delos Reyes, P. J., and Schneider, D. J.: The 1991 Pinatubo eruptions and their effects on aircraft operations, in: Fire and mud: eruptions and lahars of Mount Pinatubo, Philippines, edited by: Newhall, C. G. and Punongbayan, R. S., University of Washington Press, Seattle/London, 1071–1088, 1996.

Clarisse, L., Coheur, P. F., Prata, A. J., Hurtmans, D., Razavi, A., Phulpin, T., Hadji-Lazaro, J., and Clerbaux, C.: Tracking and quantifying volcanic SO_2 with IASI, the September 2007 eruption at Jebel at Tair, Atmos. Chem. Phys., 8, 7723–7734, doi:10.5194/acp-8-7723-2008, 2008.

Eckhardt, S., Prata, A. J., Seibert, P., Stebel, K., and Stohl, A.: Estimation of the vertical profile of sulfur dioxide injection into the atmosphere by a volcanic eruption using satellite column measurements and inverse transport modeling, Atmos. Chem. Phys., 8, 3881–3897, doi:10.5194/acp-8-3881-2008, 2008.

ACPD

11, 7757–7780, 2011

Eisinger, M. and Burrows, J. P.: Tropospheric sulfur dioxide observed by the ERS-2 GOME instrument, Geophys. Res. Lett., 25, 4177–4180, doi:10.1029/1998gl900128, 1998.
ESCAP: Review of developments in transport in Asia and the Paci?c 2005, Economic and Social Commission for Asia and the Pacific, 2005.
Guffanti, M., Casadevall, T. J., and Budding, K.: Encounters of Aircraft with Volcanic Ash Clouds: A Compilation of Known Incidents, 1953–2009, USGS, 2010.
Hjaltadóttir, S., Sigmundsson, F., Oddsson, B., Hreinsdóttir, S., Roberts, M. J., and Sveinbjörnsson, H.: Eruption in Eyjafjallajökull Status Report: 15:00 GMT, 4 May 2010, Icelandic Meteorological Office and Institute of Earth Sciences, University of Iceland, 2010.
IATA: Press Release: Volcano Crisis Cost Airlines $1.7 Billion in Revenue – IATA Urges Measures to Mitigate Impact: http://www.iata.org/pressroom/pr/Pages/2010-04-21-01.aspx, last access: 2 February 2011, 2010.
ICAO: EUR DOC 019 – Volcnic Ash Contingency Plan – EUR and NAT regions, 2nd edn., International Civil Aviation Authority, 2010.
Icelandic Met Office: Update on activity in Eyjafjallajökull: http://en.vedur.is/earthquakes-and-volcanism/articles/nr/1884, last access: 3 February 2011, 2010.
Jones, A., Thomson, D., Hort, M., and Devenish, B.: The U.K. Met Office's Next-Generation Atmospheric Dispersion Model, NAME III, in: Air Pollution Modeling and Its Application XVII, edited by: Borrego, C. and Norman, A.-L., Springer US, 580–589, 2007.
Kerr, J. B., McElroy, C.T. and Olafson, R.A.,: Measurements of Ozone with the Brewer Ozone Spectrophotometer, Proc. Int. Ozone Symposium, 74–79, 1980.
Krueger, A. J.: Sighting of El Chichon Sulfur Dioxide Clouds with the Nimbus 7 Total Ozone Mapping Spectrometer, Science, 220, 1377–1379, doi:10.1126/science.220.4604.1377, 1983.
Krueger, A. J., Walter, L. S., Bhartia, P. K., Schnetzler, C. C., Krotkov, N. A., Sprod, I., and Bluth, G. J. S.: Volcanic sulfur dioxide measurements from the total ozone mapping spectrometer instruments, J. Geophys. Res., 100, 14057–14076, doi:10.1029/95jd01222, 1995.
Pavolonis, M. J., Feltz, W. F., Heidinger, A. K., and Gallina, G. M.: A Daytime Complement to the Reverse Absorption Technique for Improved Automated Detection of Volcanic Ash, J. Atmos. Ocean Tech., 23, 1422–1444, doi:10.1175/JTECH1926.1, 2006.
Prata, A. J.: Observations of volcanic ash clouds in the 10–12 μm window using AVHRR/2 data, Int. J. Remote. Sens., 10, 751–761, 1989a.
Prata, A. J.: Infrared radiative transfer calculations for volcanic ash clouds, Geophys. Res. Lett.,

ACPD
11, 7757–7780, 2011

16, 1293–1296, doi:10.1029/GL016i011p01293, 1989b.
Prata, A. J. and Bernardo, C.: Retrieval of volcanic SO_2 column abundance from Atmospheric Infrared Sounder data, J. Geophys. Res., 112, D20204, doi:10.1029/2006jd007955, 2007.
Prata, A. J. and Grant, I. F.: Retrieval of microphysical and morphological properties of volcanic ash plumes from satellite data: Application to Mt Ruapehu, New Zealand, Q. J. Roy. Meteor. Soc., 127, 2153–2179, doi:10.1002/qj.49712757615, 2001.
Prata, A. J. and Kerkmann, J.: Simultaneous retrieval of volcanic ash and SO_2 using MSG-SEVIRI measurements, Geophys. Res. Lett., 34, L05813, doi:10.1029/2006gl028691, 2007.
Rodgers, C. D.: Inverse Methods for Atmospheric Sounding, Series on Atmospheric Oceanic and Planetary Physics, World Scientific Publishing, Singapore, 2000.
Rose, W. I., Delene, D. J., Schneider, D. J., Bluth, G. J. S., Krueger, A. J., Sprod, I., McKee, C., Davies, H. L., and Ernst, G. G. J.: Ice in the 1994 Rabaul eruption cloud: implications for volcano hazard and atmospheric effects, Nature, 375, 477–479, 1995.
Smithsonian Institution: Large explosions from the summit crater; ash plumes close airspace in Europe, BGVN, 33:04, 2010.
Stamnes, K. and Swanson, R. A.: A New Look at the Discrete Ordinate Method for Radiative Transfer Calculations in Anisotropically Scattering Atmospheres, Journal of the Atmospheric Sciences, 38, 387–399, doi:10.1175/1520-0469(1981)038¡0387:ANLATD¿2.0.CO;2, 1981.
Stohl, A., Prata, A. J., Eckhardt, S., Clarisse, L., Durant, A., Henne, S., Kristiansen, N. I., Minikin, A., Schumann, U., Seibert, P., Stebel, K., Thomas, H. E., Thorsteinsson, T., Tørseth, K., and Weinzierl, B.: Determination of time- and height-resolved volcanic ash emissions for quantitative ash dispersion modeling: the 2010 Eyjafjallajökull eruption, Atmos. Chem. Phys. Discuss., 11, 5541–5588, doi:10.5194/acpd-11-5541-2011, 2011.
Swadzba, L., Maciejny, A., Formanek, B., Liberski, P., Podolski, P., Mendala, B., Gabriel, H., and Poznanska, A.: Influence of coatings obtained by PVD on the properties of aircraft compressor blades, Surf. Coat. Tech., 78, 137–143, 1996.
Thomas, H. E., Watson, I. M., Carn, S. A., Prata, A. J., and Realmuto, V. J.: A comparison of AIRS, MODIS and OMI sulphur dioxide retrievals in volcanic clouds, Geomatics, Nat. Hazards Risk, in press, 2011.
Torres, O., Tanskanen, A., Veihelmann, B., Ahn, C., Braak, R., Bhartia, P. K., Veefkind, P., and Levelt, P.: Aerosols and surface UV products from Ozone Monitoring Instrument observations: An overview, J. Geophys. Res., 112, D24S47, doi:10.1029/2007jd008809, 2007.

ACPD
11, 7757–7780, 2011

Wen, S. and Rose, W. I.: Retrieval of sizes and total masses of particles in volcanic clouds using AVHRR bands 4 and 5, J. Geophys. Res., 99, 5421–5431, doi:10.1029/93jd03340, 1994.

Yang, K., Krotkov, N. A., Krueger, A. J., Carn, S. A., Bhartia, P. K., and Levelt, P. F.: Retrieval of large volcanic SO_2 columns from the Aura Ozone Monitoring Instrument: Comparison and limitations, J. Geophys. Res., 112, D24S43, doi:10.1029/2007jd008825, 2007.

ACPD

11, 7757–7780, 2011

Table 1. Properties of the instruments used in this study.

Instrument	Platform	Overpass Time *(local equatorial ascending)*	Field of view *(or swath width)*	Nadir Spatial Resolution
AIRS	Aqua	13:30	1650 km	14 km
GOME-2	MetOp-A	09:30	1920 km	80 × 40 km
IASI	MetOp-A	09:30	2112 km	12 km
SEVIRI	MSG	15 min sampling time	Full disk, centred: 0° N 0° E	10 km
OMI	Aura	13:45	2600 km	13 × 24 km

ACPD
11, 7757–7780, 2011

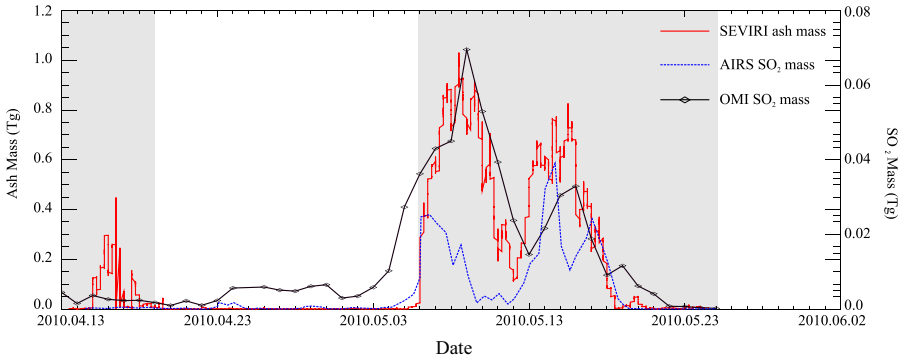

Fig. 1. Total tonnage of ash retrieved at 15 min intervals from the MSG SEVIRI instrument along with the total SO_2 mass detected by the OMI and AIRS instruments for the entire eruption period. The two shaded regions define the three different stages of the eruptive activity.

ACPD
11, 7757–7780, 2011

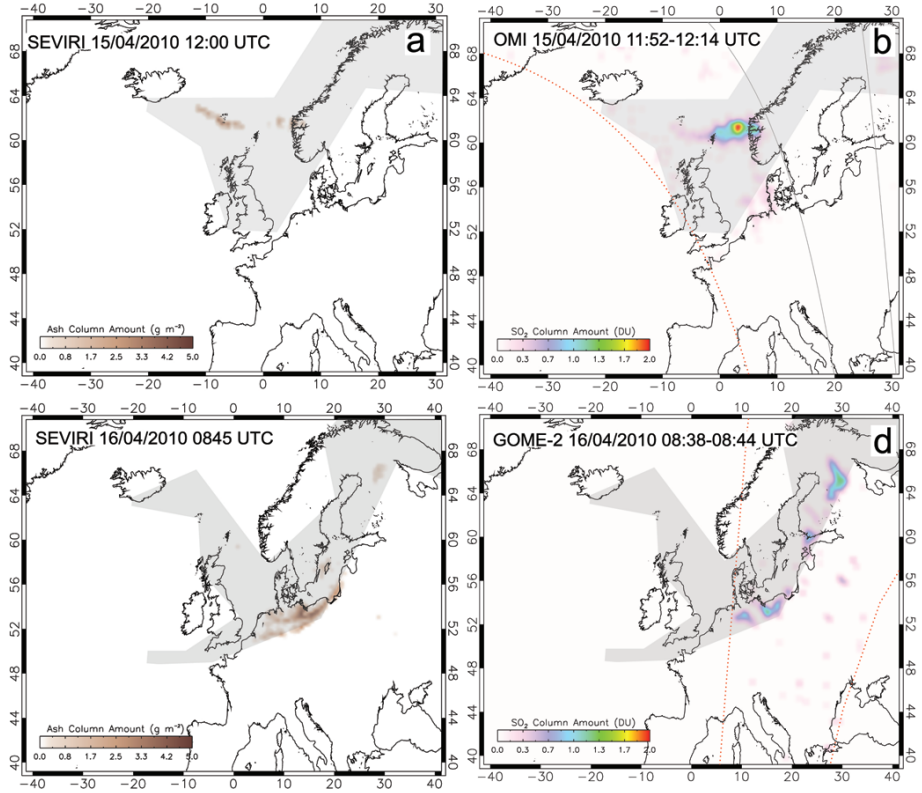

Fig. 2. Near-coincident retrieval of ash from SEVIRI with OMI SO_2 on 15 April (**a** and **b**) and with GOME-2 SO_2 data on 16 April (**c** and **d**). Red dashed lines indicate the swath edge of the polar orbiting two instruments and grey lines indicate the limit of the OMI row anomaly, between which no useable data are recorded. The grey shaded region indicates the area predicted to contain ash as forecast by the London VAAC at the time of the eruption.

ACPD
11, 7757–7780, 2011

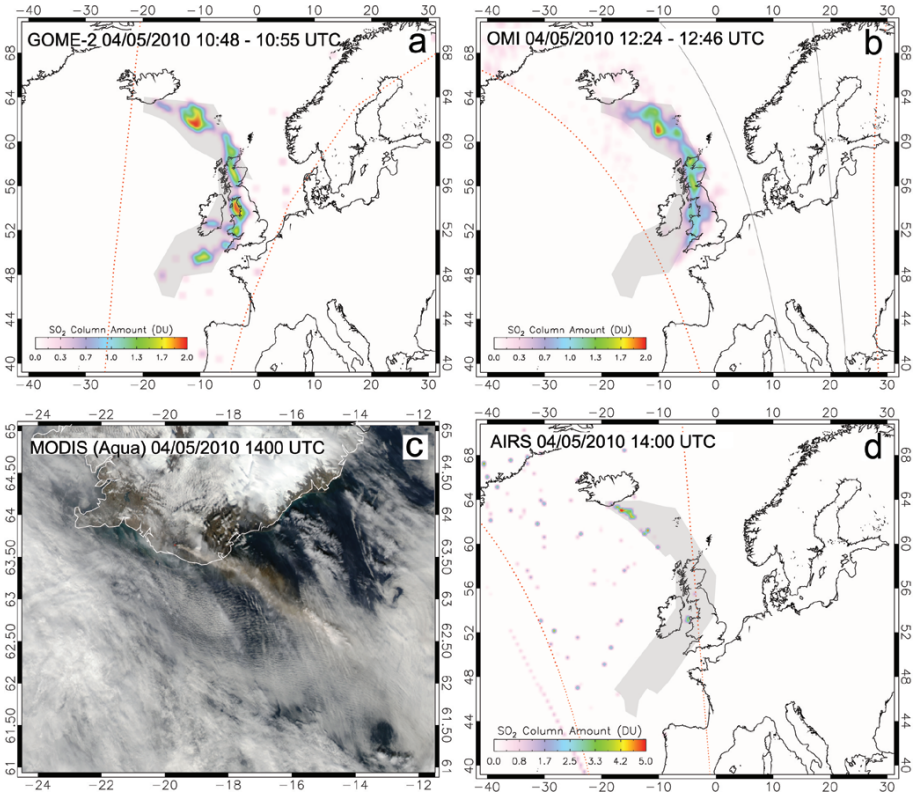

Fig. 3. SO_2 retrievals from GOME-2, OMI and AIRS on 4 May 2010 (**a**, **b** and **d**) and the visible image from the MODIS instrument on the Aqua platform showing the ash plume as it leaves the volcano. As before, red dashed lines indicate the swath edge of the polar orbiting instruments and grey lines indicate the limit of the OMI row anomaly, between which no useable data are recorded. The grey shaded region indicates the area predicted to contain ash as forecast by the London VAAC at the time of the eruption.

ACPD
11, 7757–7780, 2011

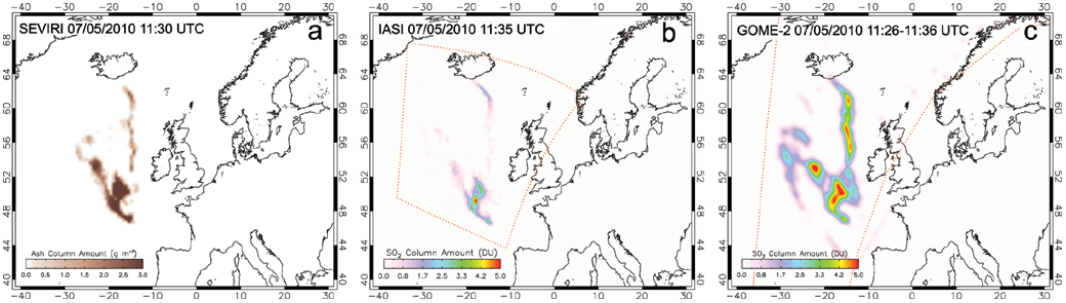

Fig. 4. Ash retrieval for 7 May 2010 from MSG-SEVIRI with the near-coincident retrievals of SO_2 from the IASI and GOME-2 instruments. As before, red dashed lines indicate the swath edge of the polar orbiting instruments (the image limit in the case of IASI).

ACPD
11, 7757–7780, 2011

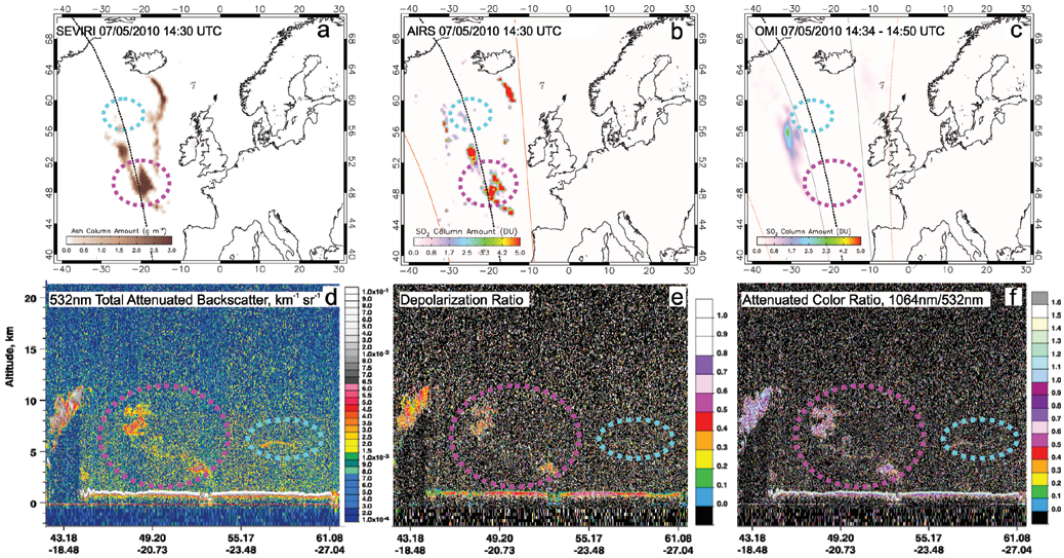

Fig. 5. Retrievals of ash and SO_2 for 7 May from SEVIRI, AIRS and OMI (**a**–**c**) as well as the coincident data from the CALIOP spaceborne lidar (**d**–**f**). The pink and turquoise circles indicate where the lidar track crosses the cloud and the associated features visible in the lidar imagery. The dashed black line defines the ground track of the lidar. As before the red dashed lines indicate the swath edge of the polar orbiting instruments and the grey lines delimit the OMI row anomaly, between which no useable data are acquired.

ACPD
11, 7757–7780, 2011

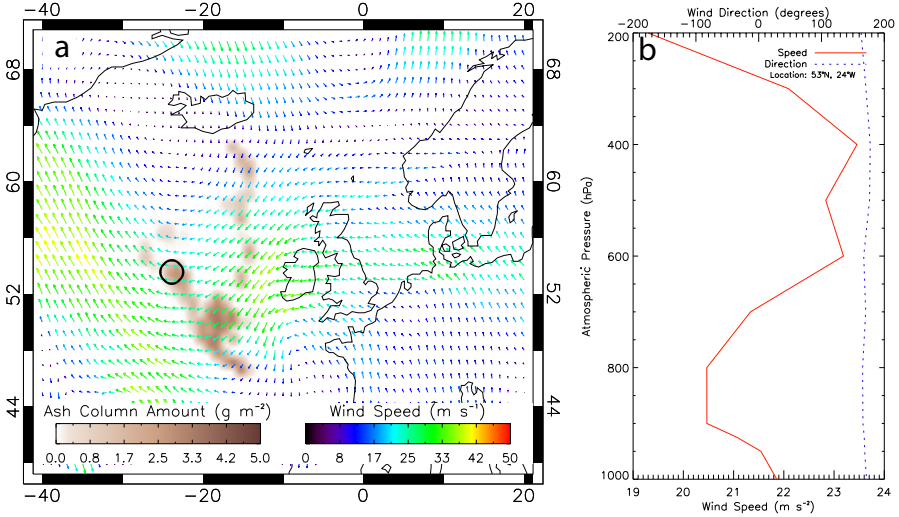

Fig. 6. **(a)** ECMWF reanalysis data for 12:00 UTC on 7 May at 500 hPa with the coincident SEVIRI ash retrieval underlain. **(b)** Vertical profile of wind speed and direction taken from the ECMWF wind data at 53° N, 24° W, location indicated by the black circle in **(a)**.

ACPD
11, 7757–7780, 2011

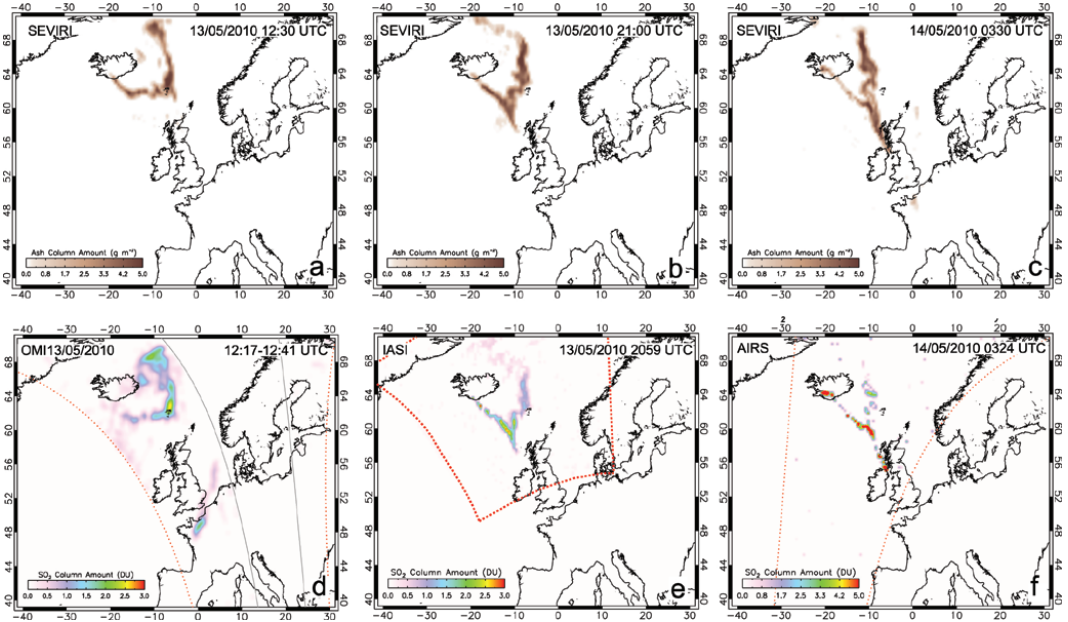

Fig. 7. Ash (**a**–**c**) from SEVIRI and SO_2 retrievals (**d**–**e**) for the latter half of 13 May and the early morning 14 May. During this time period the volcanic cloud is seen to make a dramatic change in direction. As before, red dashed lines indicate the edge of swath (or image limits in the case of IASI) of the polar orbiting instruments and the grey lines delimit the OMI row anomaly between which there are no useable data.

ACPD
11, 7757–7780, 2011

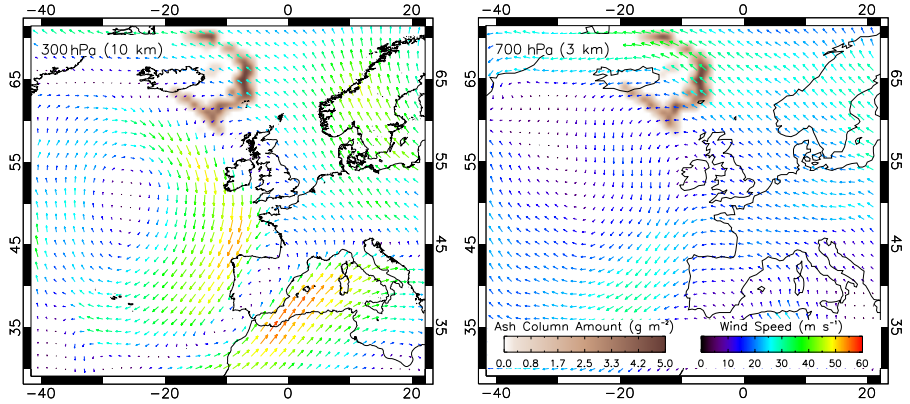

Fig. 8. ECMWF windfield data for 13 May at 18:00 UTC for the 300 hPa and 700 hPa levels (approximately 10 km and 3 km, respectively) with the coincident SEVIRI ash retrieval underlain. The windfield data shows a stronger northern component at high altitude with a stronger south-easterly windspeed at lower altitude.

ACPD
11, 7757–7780, 2011